Inversion of geomagnetic fields to derive ionospheric currents that drive geomagnetically induced currents.

J S de Villiers[1] **and P J Cilliers**[1]

[1]Space Science Directorate, South African National Space Agency, PO Box 32, Hermanus, 7200

E-mail: Jdevilliers@sansa.co.za

Abstract. Start your abstract here This research focusses on the inversion of geomagnetic field measurement to obtain source currents in the ionosphere. The ionospheric currents during a geomagnetic storm induce geo-electric fields, which in turn create geomagnetically induced currents (GICs) in power lines. These GICs may cause damage to grounded power transformers. The ultimate aim is to develop a system for predicting the ionospheric source currents from solar event data and use the link between the source currents and GICs to provide advance warning to power utilities. Line currents running East-West along given latitude are postulated to exist at a certain height above the Earth's surface. This physical arrangement expresses the fields on the ground in terms of the magnetic north and down component, and the electric east component. Ionospheric currents are modelled by inverting Fourier integrals of elementary geomagnetic fields using the Levenberg-Marquardt technique. The output parameters of the model are the current strength, height and latitude of the ionospheric current system. A conductivity structure with ten layers from Loxton, South Africa, based on the Layered-Earth model, is used to obtain the complex skin depth at a given angular frequency. The paper will present inversion results based on the Loxton structure and simulated geomagnetic fields. Model parameters can be obtained to within 2% of synthetic values. This technique has applications for modelling the currents of electrojets at the equator and auroral regions, as well as currents in the magnetosphere.

1. Introduction

Solar events, such as coronal mass ejections, that become geo-effective, creates disturbances within the Earth's magnetosphere giving rise to geo-magnetic storms and substorms. These events affect the ionospheric current systems (an example setup is given in figure 1(a)) and create fluctuations in the electric and magnetic fields on the ground. Rapid changes in the geomagnetic field generate geomagnetically induced currents (GICs) in power lines (figure 1(b)). The GICs has the potential of causing the transformers to fail, with subsequent consequences of a blackout to the general public, who are increasingly reliant on electrical power generation for their everyday operations and living.

Therefore, it is of interest to both academics and power utility operators that a warning system be developed that can predict GICs as and when an event occurs on the sun. Due to the complexities involved in such a solar-terrestrial interaction and the tremendous challenges facing such a project, we consider as a first step the inversion of the geomagnetic field observations to obtain ionospheric source currents. From these source currents we estimate the induced geo-electric fields as measured at any location of interest and the electric fields responsible for GICs in power grids on the ground.

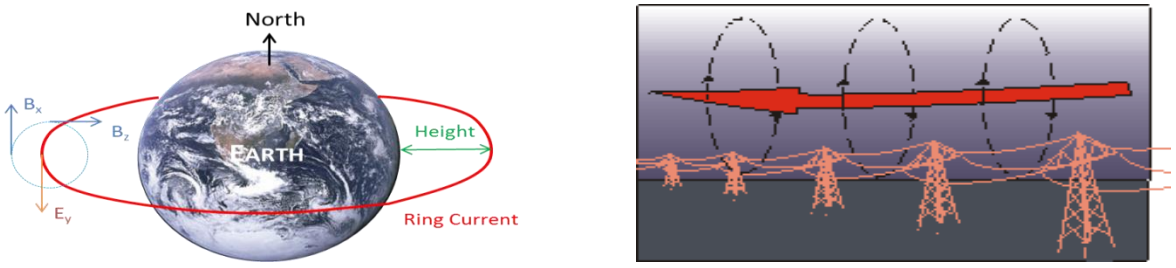

Figure 1(a): Ring current system around the Earth. **(b):** Power-lines through which GICs can be generated by fluctuations in the magnetic and electric fields.

2. Theory

2.1. Magneto-telluric Background

For a line current running in an East/West y-direction at latitude $x = 0$ and a height $z = -h$ above the Earth with a strength I, as shown in Figure 1a, the only non-zero component of the electric field is E_y (eastward). This field is determined from a diffusion equation $\nabla^2 E_y = i\sigma\omega\mu\, E_y$ in the plane-earth model [1]. The σ is the conductivity, ω is the angular frequency. The solution has both incident and reflected terms.

The magnetic field components are computed by taking the curl of this diffusion equation and using Maxwell's equations. The only non-zero components are then B_x and B_z. To relate these elementary fields to that of a line current, one must take Fourier integrals of the components and from any standard integral table, such as [2], the final form solutions of these expressions are obtained.

$$B_x(x,z) = \frac{I\mu}{2\pi}\left(\frac{h}{h^2+x^2} + \frac{h+2p}{(h+2p)^2+x^2}\right), \tag{2.1}$$

$$B_z(x,z) = -\frac{I\mu}{2\pi}\left(\frac{x}{h^2+x^2} - \frac{x}{(h+2p)^2+x^2}\right), \tag{2.2}$$

$$E_y(x,z) = -i\omega\,\frac{I\mu}{2\pi}\ln\left(\frac{(h+2p)^2+x^2}{h^2+x^2}\right)^{1/2}. \tag{2.3}$$

The skin depth $p(\omega)$ is related to the part reflected from the Earth's surface [3]. This paper diverges from [4] by studying only line current systems and replacing x with $x' = x - x_o$. This allows one to deal with the case where the current isn't vertically above the observation location, by choosing the latitude x_o of the system to be other than $x = 0$.

The complex skin depth $p(\omega)$ is computed by using a layered-earth model. The appendix of [5] describes a general approach to determine the complex surface impedance, $Z = -E_y/H_x$, from the 1D ground conductivity structure of a given location. The half-space impedance is $Z_{N+1} = K_{N+1}$. The

remaining layer impedances are calculated from a recursion relation, starting at the bottom and working all the way up to the top (that is for $n = N, \dots, 1$):

$$Z_n = K_n \frac{Z_{n+1} - K_n \tanh \lambda_n h_n}{K_n - Z_{n+1} \tanh \lambda_n h_n} \tag{2.4}$$

where $K_n = \frac{i\omega\mu_n}{\gamma_n} = \frac{(i\omega\mu_n)^{1/2}}{(\sigma_n + i\omega\varepsilon_n)^{1/2}}$ and $\gamma_n = (i\omega\mu_n)^{1/2}(\sigma_n + i\omega\varepsilon_n)^{1/2}$.

Each layer n has a thickness h_n and uniform conductivity σ_n. Once the surface impedance $Z = Z_1$ is found; it is used in the equation for the complex skin depth $p = Z/i\omega\mu_0$. In this study the permitivities is all set to $\varepsilon_n = \varepsilon_0$ and permeabilities to $\mu_n = \mu_0$.

2.2. Inversion theory

Usually we have a data set (fields) $\vec{d}$ and a model set (current, etc.) $\vec{m}$ related to each other by an operation $\boldsymbol{G}$ through the relation $\vec{d} = \boldsymbol{G}(\vec{m})$**.** We only have available the observations $\vec{d}$. The process has to be inverted for $\vec{m} = \boldsymbol{G^{-1}}(\vec{d})$ that requires optimisation techniques and an objective function**.** The optimisation is in general a non-linear least-squares fit, usually of the L_2 norm. The linear form is $\vec{m} = \boldsymbol{G^{-1}}\vec{d}$ in which case $\boldsymbol{G}$ is a matrix. In this study the Levenberg-Marquardt method were applied to this problem. This is summarized in table 1.

Table 1: Summary of the optimization setup.

Setup component	Description
The data set:	Magnetic field measurements.
The model parameters:	h = Height, x_0 = Latitude, I = Current.
The objective function:	The real and imaginary parts of magnetic field components $B_x(\omega)$, $B_z(\omega)$ and given frequency ω.
The technique:	Levenberg-Marquardt.
Derivatives	Automatically determined (Forward finite-difference).
Constraints:	None.
The performance outputs:	Iterations done, Function counts and values, Sum-of-squares residual norm, Optimality, Any messages, errors or warnings.

3. Methodology

Before optimisation can be done on determining current systems in the ionosphere, reference data were obtained against which the inversion can be tested. This was done in a forward problem using ideal current system, with given parameters and determining the fields under the current system.

Plots of impedances and skin depths and of the fields were made with respect to angular frequency in order to study its behaviour in the frequency domain. The skin depth p, or equivalently the surface impedance Z, are dependent on the frequency ω and the structure thicknesses h_i and conductivities σ_i, and therefore cannot be regarded as a model parameter. There are N levels where the $(N+1)^{\text{th}}$ level is actually the remaining half-space in plane-earth geometry with conductivity σ_{N+1} and infinite thickness.

In the optimisation the output parameter set $[I, h, x_0]$ was chosen, while keeping the structure set $[h_i, \sigma_i], i = 1, \dots, N$ plus σ_{N+1} fixed. From the field final forms, it is clear that the current strength is a linear model parameter, leading to a linear least-square inversion problem when only this parameter is adjusted for. While the placement of the height and latitude position in those field expressions turns the inversion problem into a non-linear least-squares fit.

All standard deviations are based on the Gaussian statistics of inversion theory [6]. Inversion parameter standard deviations are calculated from the Sum-of-Squares (SS) standard deviation using the Jacobian J_o of the objective function $\boldsymbol{G_i}(\vec{m}) = f(x_i; \vec{m})$ of the inversion.

A co-variance matrix is formed

$$\Sigma_\lambda = s_{SS}\left[{J_o}^T J_o\right]^{-1} \tag{3.1}$$

where the SS standard deviation is

$$s_{SS} = N^{-1} \sum_i^N {r_i}^2. \tag{3.2}$$

and the residuals is

$$r_i = d_i - \boldsymbol{G_i}(\vec{m}), \tag{3.3}$$

The variance for the parameters can then be obtained from the diagonal elements of Σ_λ. The square roots of the diagonal elements are then the parameter standard deviations.

4. Results

The 1D ground resistivity structure of Loxton, South Africa (coordinates 31^0 28' 47"S, 22^0 20' 49"E), for 10 layers is as follows: thicknesses [25,25,100,100,50,110,110,150,230,100] km, resistivities [630,10,20,30,55,40,13,4.3,2.5,0.9] Ωm. For a fixed frequency and skin depth plots of the fields vs latitude will also be shown (figure 2).

The surface impedance is $Z(\tau) = 389.7 + 976.0i$ μΩ and skin depth is $p(\tau) = 37.08 - 14.81i$ km at a fixed angular period of $\tau = 5$ minutes, or angular frequency $\omega = \frac{2\pi}{\tau} = 0.0209$ Hz. Then, using these values, one inverts the magnetic fields to obtain the best fit to the output model parameters of a line current system. The fields were first synthesised in the forward problem and a random function scaled at 10 nT added for noise before the inversion was done. The parameter values to target for were: height $h = 100$ km, latitude $x_o = 0$ km, and current strength $I = 10^6$ A. Also, the current and height were initialised at 10% above and latitude at 100 km to the north of their respective target values.

Table 2: Results from the inversion.

Model parameters	Full	Distance case 1	Distance case 1
Current $\boldsymbol{I}$ *[kA]*	$(990 \pm 2.016) \times 10^3$	$(990 \pm 2.083) \times 10^3$	$(998 \pm 2.349) \times 10^3$
Height $\boldsymbol{h}$ *[km]*	295.000 ± 0.977	295.000 ± 1.010	Fixed.
Latitude $\boldsymbol{x_o}$ *[km]*	1.620 ± 0.972	Fixed.	1.590 ± 1.144

The parameter values of the inversion are given in table 2. These three scenarios shows that all parameters stop within 1% below the values targeted for after they were initialised at 10% above the same values. This shows that the height of the current system remains the same in the first 2 cases. The latitude decreases in the last case. The current is closer to its target value. Rerunning the inversion with both distance parameters fixed leaves only the current to vary. The current obtained is $I = 10^6$ A (its target value) with a standard deviation of $\pm 3.6 \times 10^3$ A. This is even better than its fitted value in the full inversion.

In moving from the full inversion to fixing any to all parameters except one, the standard deviations among the fitted parameters are redistributing and increasing among the parameters left to vary. This is because the inversion is dealing with the same input magnetic data with errors inherent within them and displayed by their residuals. These errors are then propagated to the variances of the output parameters fitted for. So when one starts removing (fixing) a parameter from the inversion, the standard deviations of the fitting parameters that remain are expanded.

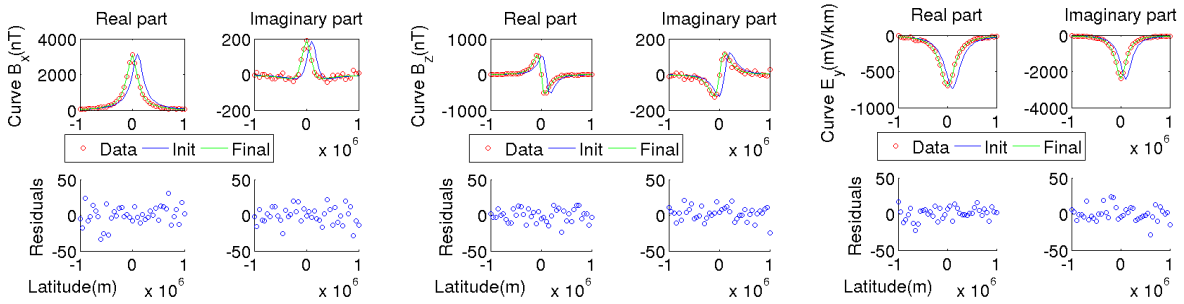

Figure2(a): Magnetic north [x-] (fitted); **(b):** Magnetic down [z-] (fitted); **(c):** Electric east [y-] (estimated).

5. Conclusions

The field plots against latitude for the chosen fixed frequency in the table, shows the expected results postulated in the forward problem. The synthetic data were used in inversion as a simulation to recover the targeted parameter values. However, due to errors introduced by a random function, the output parameters were within 1% of the given values.

As can be seen from the residual plots, the values from the fitted magnetic fields are smaller and more randomly distributed around zero. The residuals of the electric field being estimated show a similar behaviour to that for the magnetic field. This indicated that the electric field is accurate to within the error given. In practice insufficient electric field ground measurements are available. Thus, the electric field has to be excluded from the inversion procedure and can only be estimated.

These results show great promise for further investigations of current systems that are affected by events from the sun. Figure 3 shows an example of a magnetogram of the closest magnetic station to Loxton: i.e. Hermanus (latitude: 34.425°S, longitude: 19.225°E) for 31st May and 1st June 2013. The plot shows evidence of a short magnetic storm. In later investigations these real data will be Fourier analysed and then inverted in frequency space to obtain the total current strengths of multiple systems in equatorial and auroral regions within the ionosphere as well as in the magnetosphere. The approach may also apply to power lines as a current system above the ground.

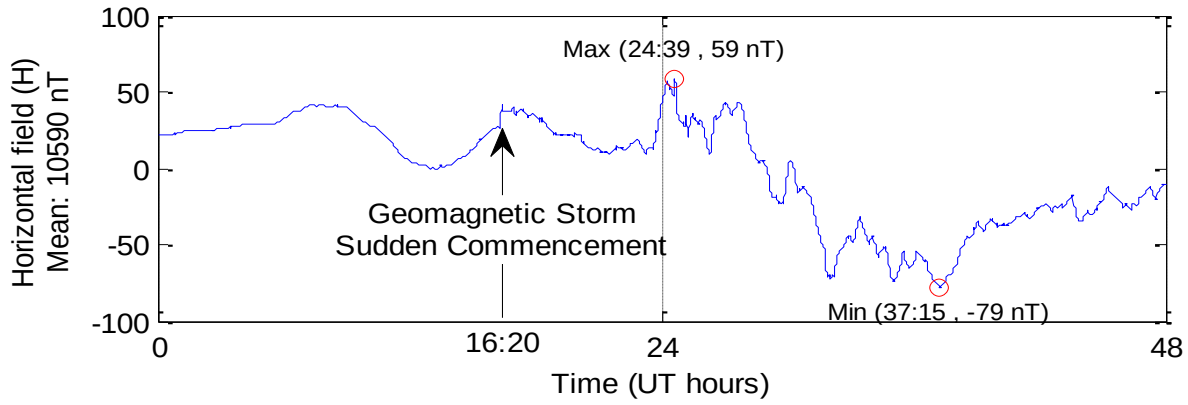

Figure 3: Magnetogram of Hermanus for 31st May and 1st June 2013.

Acknowledgements

The results presented in this poster rely on the data collected at SANSA Space Science Directorate (formerly the Hermanus Magnetic Observatory). We thank the South African National Space Agency (SANSA) for supporting its operation and INTERMAGNET for promoting high standards magnetic observatory practice (www.intermagnet.org).

References

[1] Hermance J and Peltier W 1970 Magnetotelluric fields of a line current. *J. Geophys. Res.* **75** 3351-6.

[2] Gradshteyn I and Ryzhik I 1965 *Table of integrals, Series and Products* (New York: Academic Press)

[3] Boteler D and Pirjola R 1998 The complex-image method for calculating the electric and magnetic fields produced at the surface of the Earth by the auroral electrojet. *Geophys. J. Int.* **132** 31-40.

[4] Boteler D, Pirjola R and Trichtchenko L 2000 On calculating the electrical and magnetic fields produced in technological systems at the Earth's surface by a "wide" electrojet *J. Atm. Solar-Terr. Phys.* **62** 1311-5.

[5] Wait J R 1980 Electromagnetic surface impedance for a layered earth for excitation *Radio Sci.* **15(1)** 129-34.

[6] Clifford A A 1973 *Multivariate error analysis: a handbook of error propagation and calculation in many-parameter systems* (Wiley and Sons)

[7] Evans R L, Jones A G, Garcia X, Muller M, Hamilton M, Evans S, Fourie C J S, Spratt J, Webb S, Jelsma H and Hutchins D 2011 Electrical lithosphere beneath the Kaapvaal craton, Southern Africa *J. Geophys Res.* **116** B04105.